

Electronic Delocalization in Coordination Polymers Based on Bimetallic Carboxylates

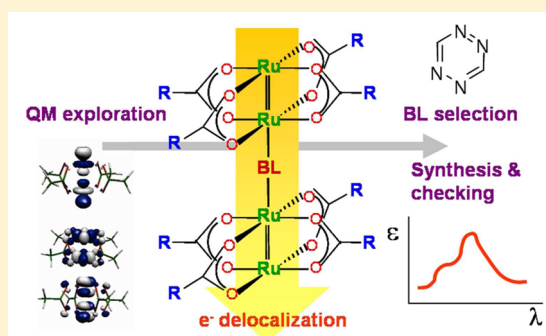
María Ana Castro,[†] Adrián E. Roitberg,^{*,‡} and Fabio D. Cukiernik^{*,†}

[†]INQUIMAE, Departamento de Química Inorgánica, Analítica y Química Física, Facultad de Ciencias Exactas y Naturales, Universidad de Buenos Aires, Pabellón II, Ciudad Universitaria, C1428EHA Buenos Aires, Argentina

[‡]Quantum Theory Project, University of Florida, Gainesville, Florida 32611, United States

S Supporting Information

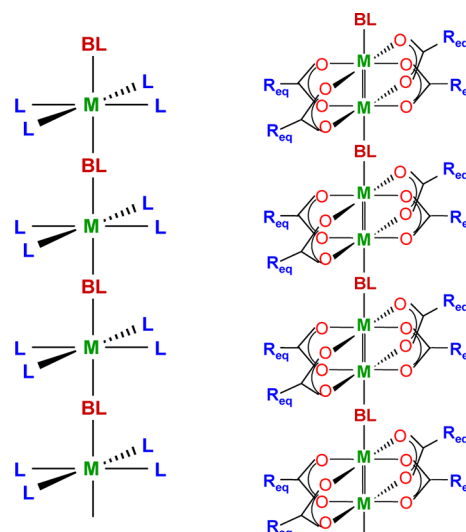
ABSTRACT: Computational methods (DFT at the B3LYP, PBE0 and m06 levels, MO fragments decomposition, and the broken symmetry approach) have been used to evaluate the influence of the bridging ligand (BL) on the extent of electron delocalization in coordination polymers based on diruthenium tetracarboxylates. The efficiency of three different nitrogenated axial ligands, namely pyrazine (pz), phenazine (phz), and tetrazine (tz), to mediate electron coupling between Ru₂(II,II) or Ru₂(II,III) centers has been estimated through four different parameters: calculated Ru–N distances, HOMO–LUMO gaps, HOMO and LUMO compositions, and magnetic coupling constants *J*. All these parameters pointed toward a coordination polymer based on Ru₂(II,II) centers axially linked by tetrazine being the best candidate for exhibiting electron delocalization through the Ru₂–BL framework. Such a compound has been synthesized and characterized; its vis–NIR spectrum exhibited the predicted features, mainly an intense low-energy MLCT band, assigned to the expected Ru₂(II,II) → tz process associated with electron delocalization.



INTRODUCTION

In this manuscript, we will investigate the issue of electronic delocalization in linear chains of bimetallic Ru carboxylates with several axial π bridging ligands; this study will be helpful for designing—at a molecular level—specific materials to be further synthesized, characterized, and studied with the midterm aim of obtaining novel liquid crystalline (LC) coordination polymers with potentiality for electronic conduction as oriented samples. Among the many attractive properties exhibited by coordination polymers (CP, Scheme 1a), the potential to transport charge along the axis of the polymer is responsible for a significant portion of the interest in these systems.^{1–7} This property depends chiefly on the electronic structure of the CP, and several mechanisms, such as hopping, are possible for the transport of charge carriers. Regardless of the mechanism, there are four key aspects to successfully develop this property in these materials: electronic structure of the metal center, geometric connectivity through the bridging ligand (BL), electronic coupling between metal centers through the BL, and the possibility of obtaining macroscopically oriented samples. The electronic structure of the metal center depends on both metal (M) and ligand (L) characteristics, as well as on the interaction between them. Geometric connectivity also depends on M and L characteristics but, more importantly, on the bridging ligand. The magnitude of the electronic coupling will be determined not only by the ML₄ center and the BL characteristics, but also by

Scheme 1



the strength of the interaction. Finally, macroscopically oriented samples appear necessary in order to either develop potential applications of CP or confidently perform physical

Received: March 7, 2013

Published: April 29, 2013

measurements. The main explored possibility is the development of single-crystals;^{4a,8} very recently, the synthesis and characterization of single strands of CP have been achieved.^{9–12}

In this context, bimetallic Ru carboxylates^{13,14} $[\text{Ru}_2(\text{O}_2\text{CR}_{\text{eq}})]_n^{n+}$ arise as promising building blocks (Scheme 1b; $L = \text{R}_{\text{eq}}\text{CO}_2^-$ = equatorial carboxylate, $n = 0$ or 1 depending on the oxidation state of the bimetallic center). First, the bimetallic center presents a potentially favorable electronic structure, since there are two available oxidation states ((II,II) and (II,III)), both with a 3-fold isoenergetic (accidentally near-degenerate) HOMO, partially filled for (II,II) derivatives and half-filled for (II,III) ones. Second, the molecular geometry is appropriate to generate 1-D extended systems provided that the axial positions are occupied by suitable bridging ligands.^{13–15} Third, it is well established that a proper selection of R_{eq} groups can generate columnar liquid-crystalline (LC) phases in these compounds, where usually these parallel columns contain a polymer chain each, parallel to the columnar axis.¹⁶ In some cases, these LC phases are stable at room temperature, and their moderate viscosity has led to macroscopically oriented samples extruded into fibers,¹⁷ an incipient orientation technique for LC pseudo-CP¹⁸ or CP.¹⁹

With this background, we decided to deepen the study of electronic coupling between bimetallic centers through the bridging ligand, in order to establish the basis for a rational design of a CP based on these building blocks. To choose the most promising bimetallic center-bridging ligand combination, we decided to start with a computational exploration of suitable candidates. *A priori* computational studies on $\text{Ru}_2(\text{O}_2\text{CR})_4 \dots \text{Ru}_2(\text{O}_2\text{CR})_4$ communication have been previously carried out only for equatorially linked mixed-valence systems²⁰ and for one axially bridged divalent system: $\text{Ru}_2(\text{O}_2\text{CCH}_3)_4\text{pz}$ studied by Hückel methods.²¹ Electronic coupling between related paddle-wheel diruthenium units has also been studied for discrete molecular systems; in these cases, *a posteriori* computational studies helped the interpretation of experimental results.^{22,23}

¹H NMR studies on several of these paramagnetic Ru_2 species showed that the unpaired π^* electrons on the Ru_2 unit can be partly delocalized on axial π ligands.²³ On this basis, we could expect that the use of bridging ligands such as pyrazine (pz), phenazine (phz), or tetrazine (tz) could lead to good communication between bimetallic units. In turn, the resulting relatively rigid structure should favor the formation of linear chains and single-dimensional arrays. A certain number of polymeric bimetallic tetracarboxylates containing these bridging ligands has been synthesized and characterized,^{24–32} and in every case, the bimetallic core remained intact upon polymerization.

Pyrazine was chosen in particular because this is a prototypical ligand in the coordination chemistry field as bridge for electron delocalization. Some compounds have already been synthesized and characterized such as those in which $\text{Ru}_2(\mu\text{-O}_2\text{CCH}_3)_4^+$,^{24,26} $\text{Ru}_2(\mu\text{-O}_2\text{CCH}_3)_4$,²⁷ or $\text{Ru}_2(\mu\text{-O}_2\text{CC}(\text{CH}_3)_3)_4$ ³² bimetallic units are bridged by axial pyrazine. However, communication was usually not good, and they showed very weak antiferromagnetic (AF) interactions between the bimetallic units (in addition to the well established zero-field splitting all these compounds exhibit)³³ and, in some cases, did not show any interaction at all.^{26,27,32} Indeed, analysis of this magnetic interaction within the framework of the mean molecular field approximation gave $zJ = -2.3 \text{ cm}^{-1}$ for $[\text{Ru}_2(\mu\text{-O}_2\text{CCH}_3)_4(\text{pz})]_n(\text{BPh}_4)_n^{24}$ and $zJ = -3.12 \text{ cm}^{-1}$ for $[\text{Ru}_2(\mu\text{-O}_2\text{CC}(\text{CH}_3)_3)_4(\text{pz})]_n(\text{BPh}_4)_n$.³² (As previously stated by Maldivi et al.,³⁴ zJ values obtained by refinement of magnetic data for the analogous divalent compounds exhibiting weak magnetic interactions are subjected to great uncertainty—due to the nature of the ground magnetic state populated at low temperatures in these compounds exhibiting a very large zero-field splitting—and should be taken with care.)

Phenazine was chosen, as it presents a more extended aromatic system which results in a lower energy π^* orbital that could lead to a smaller HOMO–LUMO gap and greater interaction between the Ru_2 centers. Moreover, as there are structurally characterized compounds, namely those based on $\text{Ru}_2(\mu\text{-O}_2\text{CC}_2\text{H}_5)_4^+$,²⁹ $\text{Ru}_2(\mu\text{-O}_2\text{CC}(\text{CH}_3)_3)_4^+$,³² and $\text{Ru}_2(\mu\text{-O}_2\text{CCF}_3)_4$,³⁰ the experimental geometries of these are used as a reference for comparison with the optimized geometries resulting from the calculations.

Finally, tetrazine was included since the presence of four N atoms in the ring results in a low energy π^* unoccupied orbital,³⁵ making tz a very promising ligand for achieving good communication between the Ru_2 units. In fact, this feature has already been exploited in other systems of coordination polymers with high conductivity along the axis.^{7,35–42}

We decided to include the two possible Ru centers, $\text{Ru}_2(\text{II,III})$ and $\text{Ru}_2(\text{II,II})$. The former is easier to manipulate from the experimental point of view but shows a lower energy half-filled HOMO, which therefore could result in both a poor orbital interaction with the axial ligand and a greater tendency to exhibit Peierls distortion. On the other hand, the latter, which requires an inert atmosphere at least during the stages of synthesis in solution, presents a higher energy 2/3-filled HOMO and could thus overcome the disadvantages of (II,III) species.

As we are interested at this stage in a comparison of the interaction of the diruthenium centers through the axial bridging ligands, calculations have been performed on “dimers of dimers” tetranuclear models, an often used approach for CP based on bimetallic units.^{21,43,44} The main parameters considered in the present computational exploration as estimators of the strength of this interaction were the HOMO–LUMO gap, the Ru–N distance, the HOMO and LUMO composition, and the magnetic coupling between centers. The HOMO–LUMO gap in these discrete models provides insight on the band gap that the extended systems could exhibit, under the assumption that the involved MOs effectively give rise to a band structure; the composition of these MOs is informative about the degree of mixing of Ru_2 -centered and BL-centered MOs. Ru–N distance is the main geometric parameter that presents a strong correlation with this interaction; the magnetic coupling constant J provides an estimation of this interaction which can be experimentally measured (for this reason, it has been preferred over other parameters usually used for estimating electronic communication, like hopping integrals). To evaluate them, DFT(B3LYP/LanL2DZ) calculations and the broken symmetry approach were used, as they are previously validated methodologies for the study of transition metal–carboxylate complexes, that we successfully used to account for experimental trends in physicochemical properties of a homologous series of $[\text{Ru}_2(\mu\text{-O}_2\text{CCH}_3)_4\text{X}_2]^-$ ($\text{X} = \text{Cl}, \text{Br}, \text{I}$),⁴⁵ to explain some structural aspects of polymers $[\text{Ru}_2(\text{O}_2\text{CR})_4\text{Cl}]_\infty$,⁴⁵ as well as to interpret the magnetic properties of a related hexanuclear Cu cluster.⁴⁶

On the basis of this computational exploration, we synthesized a polymeric $\text{Ru}_2(\text{O}_2\text{C}(\text{CH}_2)_2\text{CH}_3)_4\text{BL}$ compound, which exhibited the essential features predicted by our calculations.

COMPUTATIONAL METHODS

Theoretical calculations were performed with density functional theory (DFT) as implemented in the Gaussian 03 and Gaussian 09 packages.⁴⁷ Unless otherwise stated, we used Becke's three parameter hybrid functional with the correlation functional of Lee, Yang, and Parr formalized as the B3LYP hybrid functional (20% Fock exchange).⁴⁸ Unrestricted open-shell calculations were performed in every case. An effective core potential basis set LanL2DZ⁴⁹ was used as it presented the better compromise between accuracy and computational cost. All structures were fully optimized, and harmonic frequency calculations were performed to establish the nature of the critical points (minimum or transition state). No symmetry constraints were used for the optimization. Calculations at fixed geometry were then performed in order to test the effect of different functionals: the PBE0⁵⁰ and Truhlar's m06⁵¹ functionals that account for 25 and 27% Fock exchange were considered.

The energies and intensities of the lowest 200 singlet–singlet electronic transitions were calculated with TD-DFT,⁵² which covered the region up to 250 nm (B3LYP). The UV–vis spectra were plotted using the SWizard⁵³ program, using a Gaussian broadening model. The half-bandwidths were taken to be equal to 3000 cm^{-1} . Molecular structures and orbitals were visualized with the program MOLEKEL.⁵⁴

We employed the broken symmetry formalism, originally developed by Noodleman for SCF methods,⁵⁵ which involves a variational treatment within the restrictions of a single spin-unrestricted Slater determinant built upon using different orbitals for different spin. This approach was later applied within the frame of DFT. We preferred the use of the approximation described by Yamaguchi and co-workers⁵⁶ to link the exchange coupling parameter with the energies and expectation values of the spin-squared operator for the HS and BS states.^{56,57}

$$J = - \frac{E_{\text{HS}} - E_{\text{BS}}}{\langle \hat{S}_{\text{HS}}^2 \rangle - \langle \hat{S}_{\text{BS}}^2 \rangle} \quad (1)$$

EXPERIMENTAL SECTION

Synthesis of $[\text{Ru}_2(\text{O}_2\text{C}(\text{CH}_2)_2\text{CH}_3)_4]\text{tz}_2$ and $[\text{Ru}_2(\text{O}_2\text{C}(\text{CH}_2)_2\text{CH}_3)_4]\text{tz}$. Both compounds have been synthesized by solution reaction of ruthenium butanoate, $\text{Ru}_2(\text{O}_2\text{C}(\text{CH}_2)_2\text{CH}_3)_4$, with tetrazine, in stoichiometric amounts. Tetrazine has been synthesized after ref 58 and ruthenium butanoate by Cr(II) reduction of $\text{Ru}_2(\text{O}_2\text{C}(\text{CH}_2)_2\text{CH}_3)_4\text{Cl}$ following Maldivi et al.'s procedure.⁵⁹ Synthetic details for each compound are given below. All the described syntheses have been carried out under a N_2 atmosphere, using a Braun LabMaster 130 glovebox; solvents were dried and deoxygenated following usual procedures.

$\text{Ru}_2(\text{O}_2\text{C}(\text{CH}_2)_2\text{CH}_3)_4\text{Cl}$. Following the procedure described in Virelizier et al.,⁶⁰ 500 mg of $\text{Ru}_2(\text{O}_2\text{C}(\text{CH}_2)_2\text{CH}_3)_4\text{Cl}$ and 30 mL of butyric acid were mixed and kept to reflux. The solid dissolved completely after approximately 15 min, yielding a dark solution. After additional 15 min, the system was left to cool to room temperature; then the bright violet microcrystalline precipitate was filtered, washed with *n*-heptane and then with petroleum

ether, and finally dried under vacuum. %C exptl. (calcd.): 32.6 (32.8). %H exptl. (calcd.): 5.2 (4.8).

$[\text{Ru}_2(\text{O}_2\text{C}(\text{CH}_2)_2\text{CH}_3)_4]\text{tz}_2$. A total of 174 mg of $\text{Ru}_2(\text{O}_2\text{C}(\text{CH}_2)_2\text{CH}_3)_4$ was dissolved in CH_2Cl_2 and added dropwise with agitation to a solution of 52 mg of tetrazine in CH_2Cl_2 , resulting in a violet solution. Due to its low molecular weight, tetrazine is a very volatile compound that sublimates at room temperature; thus its excess was easily eliminated through evaporation (reddish fumes were observed): %C exptl. (calcd.): 32.5 (33.6). %H exptl. (calcd.): 4.4 (4.5). %N exptl. (calcd.): 15.4 (15.7).

$[\text{Ru}_2(\text{O}_2\text{C}(\text{CH}_2)_2\text{CH}_3)_4]\text{tz}$. A total of 33 mg of $\text{Ru}_2(\text{O}_2\text{C}(\text{CH}_2)_2\text{CH}_3)_4$ was dissolved in CH_2Cl_2 and added dropwise with agitation to a solution of 5 mg of tetrazine in CH_2Cl_2 , resulting in a violet solution. No excess tetrazine (no reddish fumes) were observed through evaporation. %C exptl. (calcd.): 32.8 (34.2). %H exptl. (calcd.): 4.8 (4.8). %N exptl. (calcd.): 7.8 (8.9).

Physicochemical Measurements. Elemental analyses were carried out at *Servicio a Terceros* of INQUIMAE, on a Carlo Erba CHNS-O EA1108 analyzer. UV–vis–NIR spectra were acquired using a diode array HP8453A spectrophotometer; quartz cells were filled inside the glovebox, firmly covered and measured within a few minutes. Appreciable spectral changes have only been detected after periods longer than 1 h. Solutions were prepared with dry degassed solvents.

RESULTS

The values calculated for the Ru–N distance, the HOMO–LUMO gap, and the magnetic exchange constant J calculated by broken symmetry are collected in Table 1. Additional

Table 1. Calculated Values for the Optimized Ru–N Distance for $[\text{Ru}_2(\mu\text{-O}_2\text{CCH}_3)_4\text{L}]_2\text{L}^{2+}$ (Noted (II,III)-L) and $[\text{Ru}_2(\mu\text{-O}_2\text{CCH}_3)_4\text{L}]_2\text{L}$ (Noted (II,II)-L) for $L = \text{pz}$, phz , and tz^a

compound	$d_{\text{Ru-N}}$ (Å)	HOMO–LUMO gap (eV)			zJ (cm^{-1})		
		B3LYP	PBE0	M06	B3LYP	PBE0	M06
(II,III)-pz	2.256	4.1	4.2	3.9	−1.1	−0.7	−2.0
(II,III)-phz	2.385	2.7	3.1	2.9	−1.1	−1.1	−1.4
(II,III)-tz	2.273	2.6	2.6	2.4	−0.9	−0.2	−3.2
(II,II)-pz	2.317	3.0	3.4	3.2	−8.7	−7.6	−4.1
(II,II)-phz	2.475	2.6	2.9	2.7	−2.1	−2.1	−3.7
(II,II)-tz	2.138	1.9	2.5	1.8	−15.1	−14.5	−5.0

^aThe HOMO–LUMO gap and the magnetic coupling constant J calculated with the three functionals are shown. Additional details are included in Tables S5–S8.

information on the main parameters for the optimized geometries is given in Tables S1–S4. It is important to highlight the match between the calculated and experimental geometries in the case of phz (Figures S1 and S2).

Results obtained with the B3LYP and PBE0 functionals are almost identical for both HOMO–LUMO gaps and zJ estimations. When considering the m06 functional, although the HOMO–LUMO gaps are very similar to those obtained with the other functionals, slight differences are observed for the absolute zJ values. However, the general trend is the same in every case and the largest values are observed for the same compounds. Therefore, we conclude that there is no significant

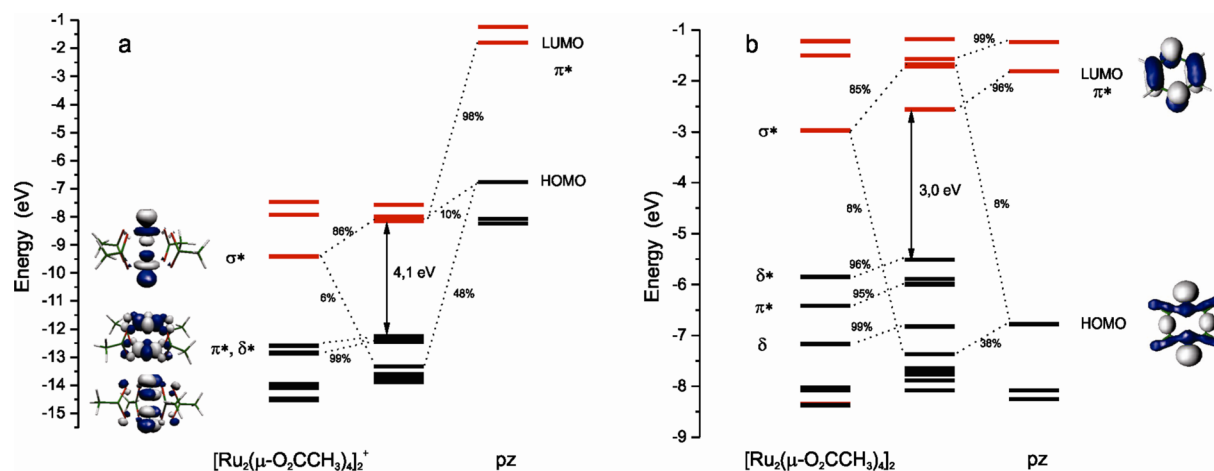


Figure 1. MO diagrams for the pyrazine-bridged compounds: (a) $[\text{Ru}_2(\mu\text{-O}_2\text{CCH}_3)_4]_2\text{pz}^{2+}$, (b) $[\text{Ru}_2(\mu\text{-O}_2\text{CCH}_3)_4]_2\text{pz}$. Occupied MOs are shown in black and unoccupied MOs in red.

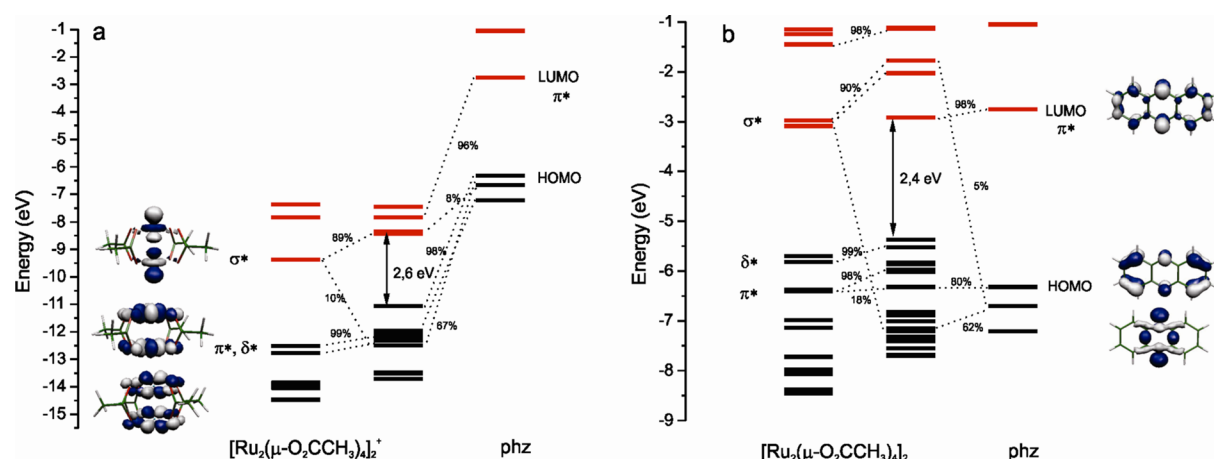


Figure 2. MO diagrams for the phenazine-bridged compounds: (a) $[\text{Ru}_2(\mu\text{-O}_2\text{CCH}_3)_4]_2\text{phz}^{2+}$, (b) $[\text{Ru}_2(\mu\text{-O}_2\text{CCH}_3)_4]_2\text{phz}$. Occupied MOs are shown in black and unoccupied MOs in red.

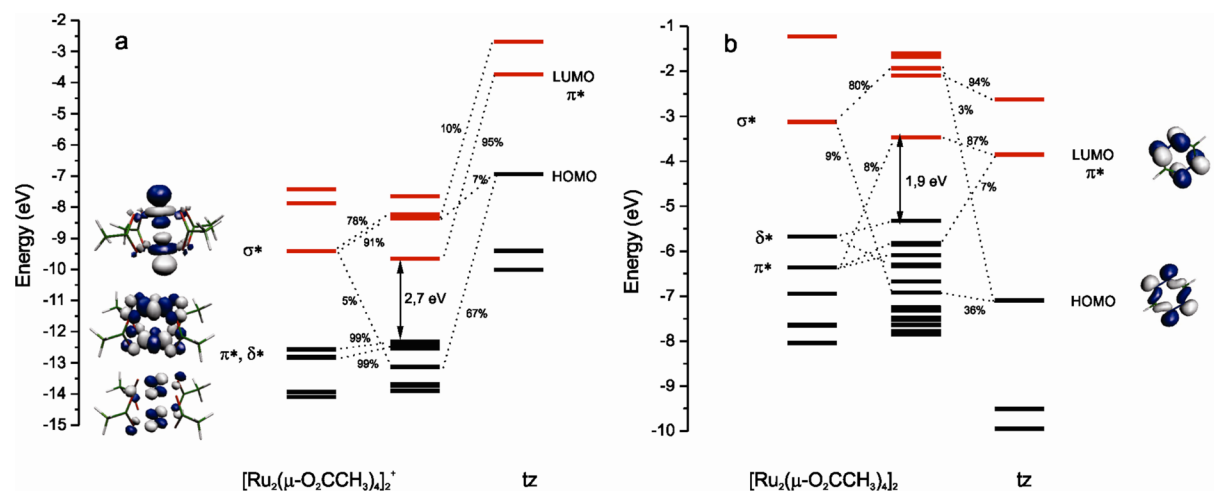


Figure 3. MO diagrams for the tetrazine-bridged compounds: (a) $[\text{Ru}_2(\mu\text{-O}_2\text{CCH}_3)_4]_2\text{tz}^{2+}$, (b) $[\text{Ru}_2(\mu\text{-O}_2\text{CCH}_3)_4]_2\text{tz}$. Occupied MOs are shown in black and unoccupied MOs in red.

functional effect on the predicted trend for the magnetic coupling constant and from here on will discuss the B3LYP results for simplicity.

Our calculations predict, for both (II,III) and (II,II) derivatives, longer Ru–N distances for phenazine derivatives

than for pyrazine or tetrazine ones, a fact certainly related to the steric hindrance. The shortest distance found in the calculations is 2.138 Å for (II,II)-tz. The HOMO–LUMO gap for mixed-valence derivatives varies from a high value for (II,III)-pz (4.1 eV) to moderate values for both (II,III)-phz and (II,III)-tz (2.7

and 2.6 eV, respectively). For divalent derivatives, the predicted trend is more pronounced: a monotonic variation from a high 3.0 eV value for (II,II)-pz to a low 1.9 eV value found for (II,II)-tz, the lowest value calculated among these compounds. At a first level of analysis, both geometric and energetic aspects point toward (II,II)-tz exhibiting the highest degree of electronic delocalization. However, the extrapolation of the HOMO–LUMO gap from these discrete systems to their extended analogues, as well as the interpretation of its variation along each series, is not straightforward and requires more detailed information about the nature of the involved MOs.

In order to gain a better understanding of the electronic structure of these species, single point calculations were made for both “dimers of dimers” and the various fragments in order to calculate the fragment’s MO contribution to the “dimer of dimers” MOs through the program AOMIX.^{61,62} For this, we used the geometry optimized for each tetranuclear system. Figures 1–3 show the MO diagrams calculated for the six compounds. Additional details are provided as Supporting Information (Tables S9–S14).

Comparison of these MO diagrams with the only previously calculated one for (II,II)-pz by the Hückel method²¹ shows some significant discrepancies, expected due to the increased complexity of the methodology used in this case. The main one is the larger HOMO–LUMO gap calculated in the present study (3.0 vs 1.1 eV); our result seems to agree with experimental evidence that points toward weak electron delocalization along the polymeric $[\text{Ru}_2\text{-pz}]_n$ chain.

An inspection of the MO diagrams of the mixed valence complexes shows no significant orbital interactions at the frontier MO level. Indeed, for both (II,III)-pz and (II,III)-tz, HOMO to HOMO–5 are 99% composed of π^* and δ^* MOs of the binuclear units; a similar situation is found for (II,III)-phz, with the only difference that they appear as HOMO–2 to HOMO–3 and HOMO–5 to HOMO–8, due to the intercalation of nearly pure phz MOs. The BL-LUMOs, on the other hand, are retrieved as essentially unmixed MOs in the respective “dimers of dimers” (LUMO+2, LUMO+2 and LUMO+0 for (II,III)-pz, (II,III)-phz and (II,III)-tz, respectively; in the first two cases, LUMO+0 and LUMO+1 correspond to σ^* MOs essentially belonging to the dimetallic centers). Thus, the MO scheme for the three mixed valence tetranuclear units correspond essentially to those of the metal–metal bond of each dinuclear unit, showing orbital interactions with BL only at a σ level. The trend in the HOMO–LUMO gap along this series should clearly be analyzed with some care, as it corresponds to $\delta^*(\text{Ru}_2)\text{-}\sigma^*(\text{Ru}_2)$, $\pi(\text{BL})\text{-}\sigma^*(\text{Ru}_2)$, and $\delta^*(\text{Ru}_2)\text{-}\pi^*(\text{BL})$ for (II,III)-pz, (II,III)-phz, and (II,III)-tz, respectively. On the other hand, for the same reason, it is not a good estimator of the expected band gap trend for extended systems, as the involved MOs don’t necessarily give rise to bands to the same extent. However, it should be noticed that although the tz-LUMO is still higher in energy than the complex’s MOs, it presents a lower energy than pz-LUMO and phz-LUMO; consequently, the interaction is more effective than in the other cases, yielding a BL-centered LUMO (95%) for the tetranuclear moiety.

For the three divalent compounds studied, the energy difference between the MO of the fragments is lower than in the mixed valence series, as expected given that the charge on the complex is zero, and this results in a smaller HOMO–LUMO gap for the (II,II) series. Moreover, the nature of both HOMO and LUMO is the same along the (II,II)-BL series:

HOMO–0 to HOMO–5 are essentially π^* and δ^* MOs of the binuclear units, while the LUMO is essentially BL-based. The nature of these frontier MOs ensure a physically meaningful evaluation of the HOMO–LUMO gap in the terms described above and allows for an interpretation of the trend. Indeed, the decrease found in the HOMO–LUMO gap from (II,II)-pz to (II,II)-phz could be ascribed to the lower energy of the phz-LUMO with respect to the pz-LUMO, although the Ru–N distance is longer for the phenazine derivative. The HOMO–LUMO gap calculated for the tetrazine analog, (II,II)-tz, is the lowest of the studied compounds. This is certainly due to both the lower energy of the tz-LUMO and the shorter Ru–N distance that the (II,II)-tz compound is predicted to exhibit. Both factors increase the Ru_2 –BL MO interactions. Indeed, an analysis of the composition of the MO for this compound shows that it exhibits the highest degree of mixing: the LUMO of (II,II)-tz is 87% tz-LUMO and 8% $\text{Ru}_2\text{-}\pi^*$; the HOMO MO of (II,II)-tz also contains some contribution from the BL-MO.

The analysis of the magnetic interaction, a measurable physical property useful as an estimate of the electronic coupling through the bridging ligand, agrees with the electronic structure trends just discussed. All the studied mixed-valent systems present weak antiferromagnetic interactions of roughly the same order of magnitude. The values obtained for zJ are -1.1 cm^{-1} , -1.1 cm^{-1} , and -0.9 cm^{-1} for pz, phz, and tz, respectively. Given the small size of the interaction, it is not possible to obtain reliable quantitative results for these compounds, but some qualitative conclusions can be drawn. The results are consistent with the experimental values of -2.3 cm^{-1} and -3.1 cm^{-1} found for pyrazine compounds^{26,32} and of -1.5 cm^{-1} and -0.65 cm^{-1} for phenazine compounds.³² In the first case, the poor communication between centers seems to be due to a difference in energy between the orbitals centered on the Ru_2 moiety and the ones centered on the bridging ligand. In the second case, it seems to be the result of the longer Ru–N distance caused by phenazine’s steric hindrance rather than an energy mismatch. An increase in the magnetic interaction is not predicted for the tetrazine derivative. This is striking because, as compared to pz, it presents a smaller HOMO–LUMO gap and a similar Ru–N distance, which should result in a greater coupling constant J ; as compared to phz, it has a similar HOMO–LUMO gap and a smaller Ru–N distance, which should also result in greater J . While it is not possible to suggest a definitive explanation of this fact, it is probably a result of the three interactions being very weak, and about the same magnitude, so this method does not allow discriminating quantitatively from one another.

The situation is different for the analyzed $\text{Ru}_2(\text{II,II})$ compounds, as significant variations of the calculated antiferromagnetic coupling zJ is observed along the series. The value found for pyrazine (-8.7 cm^{-1}) is greater than the one obtained for the mixed-valent analog, a fact certainly related to the orbital energies, as discussed above. In the case of phenazine, which has a slightly smaller HOMO–LUMO gap and longer Ru–N distance than the pz compounds, the calculated zJ value was -2.1 cm^{-1} , higher than that for the corresponding (II,III) analog, but smaller than for the pz/(II,II) compound. This is consistent with what was expected and shows that systems with phz as a bridging ligand are not appropriate when looking for a good electronic communication between bimetallic centers, as previously discussed on experimental bases. Incidentally, taking into account the inherent difficulty in assessing an experimental value of the

antiferromagnetic exchange in these zero-field split $\text{Ru}_2(\text{II,II})$ systems, the present calculations seem to qualitatively validate the value obtained by refinement of the experimental data (e.g.: $zJ = -3.0 \text{ cm}^{-1}$ for $\text{Ru}_2(\text{O}_2\text{CCF}_3)_4\text{phz}$).³⁰ For the tetrazine compound, a J value of -15.1 cm^{-1} was calculated. This represents the largest magnetic coupling obtained and is consistent with the fact that not only the HOMO–LUMO gap is smaller and the MO mixing is higher than the in rest of the systems studied but also the Ru–N distance is very small, only 2.138 Å.

Both electronic and structural factors suggest that, among the studied series, tetrazine- $\text{Ru}_2(\text{II,II})$ compounds should exhibit the largest degree of communication between bimetallic centers through the bridging ligand. On this basis, we decided to synthesize a polymer with this bimetallic center and tetrazine as a bridging ligand. We choose the energy and intensity of the expected MLCT band corresponding to the lowest energy $\text{Ru}_2 \rightarrow \text{tz}$ transition as experimental data sets to validate our predictions. Alternative choices, like the magnetic exchange coupling or the electric conductivity, were discarded: the first one, due to the uncertainty associated with its determination in this highly zero-field split systems, as discussed above, and the second one, because it requires oriented samples, still unavailable at this stage. Qualitatively, the predicted significant Ru_2 –BL interaction for (II,II)-tz, associated to a moderate MO mixing and a low HOMO–LUMO gap, should give rise to low energy $\text{Ru}_2 \rightarrow \text{tz}$ absorption bands with significant intensity. TD-DFT calculations performed on both a bis-adduct $\text{Ru}_2(\text{II,II})$ /tetrazine compound and a “dimer of dimers” (taken again as a model for the CP) confirmed this prediction: as expected, their calculated spectra (Figure S3) show an intense band in the NIR region, which is predominantly $\pi^*(\text{Ru}_2) \rightarrow \pi^*(\text{tz})$ and $\sigma^*(\text{Ru}_2) \rightarrow \pi^*(\text{tz})$ in character.

Two different solids, a bis-adduct $[\text{Ru}_2(\text{O}_2\text{C}(\text{CH}_2)_2\text{CH}_3)_4]\text{-tz}_2$ and polymeric $[\text{Ru}_2(\text{O}_2\text{C}(\text{CH}_2)_2\text{CH}_3)_4]\text{tz}$, have been synthesized by solution reaction of $[\text{Ru}_2(\text{O}_2\text{C}(\text{CH}_2)_2\text{CH}_3)_4]$ with stoichiometric amounts of tetrazine and isolated as purple solids (details on the synthesis and characterization have been given in the Experimental Section). Their vis/NIR spectra in dichloromethane (shown in Figure 4) exhibit three main bands,

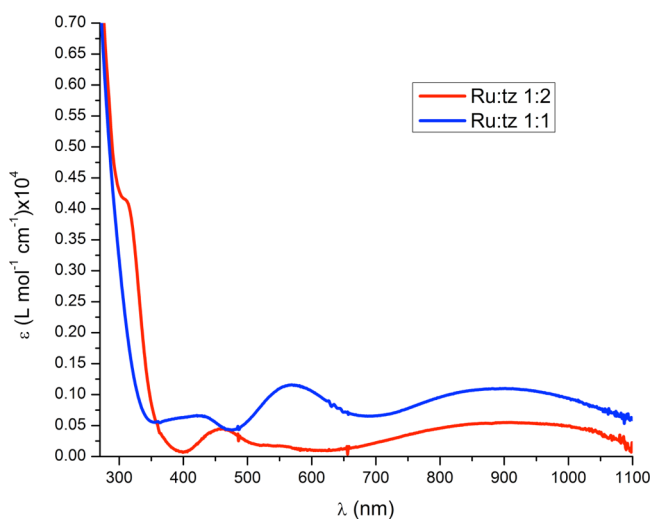


Figure 4. UV–vis spectra in CH_2Cl_2 for the two different (II,II)-tz compounds synthesized: $[\text{Ru}_2(\mu\text{-O}_2\text{C}(\text{CH}_2)_2\text{CH}_3)_4]\text{tz}$ (blue line) and $[\text{Ru}_2(\mu\text{-O}_2\text{C}(\text{CH}_2)_2\text{CH}_3)_4]\text{tz}_2$ (red line).

with slight differences in their energies and relative intensities. The first one, at 463 nm for the bis-adduct 1:2 species and at 421 nm for the 1:1 species, is assigned to the well-established $\pi_{\text{Ru-O}} \rightarrow \pi^*(\text{Ru}_2)$ transition typical of diruthenium carboxylates. The medium energy one (at 552 nm for the 1:2 species; 569 nm for the 1:1 polymer) contains both $\pi_{\text{Ru-O}} \rightarrow \pi^*(\text{Ru}_2)$ and MLCT components, according to our TD-DFT calculations (Table S15). Finally, a low energy wide band centered at ca. 880 nm is observed for both compounds. This band, absent in pyrazine derivatives, can be assigned to the expected MLCT band.

CONCLUSIONS

In conclusion, our calculations on molecular geometries, HOMO–LUMO gaps, and compositions as well as on magnetic exchange constants of two series of diruthenium compounds linked by three different bridging ligands pointed toward the (II,II)-tetrazine system as the most suitable candidate for exhibiting electronic delocalization through the bridging ligand. The vis/NIR spectrum of a synthesized polymeric system validated our computational prediction. Studies aimed to synthesize LC analogs of this CP suitable for being processed as macroscopically oriented samples, then to measure their electric conductivity, are currently underway in our lab.

ASSOCIATED CONTENT

Supporting Information

Tables and figures with bond distances, bond angles, electronic structures, and calculated optical transitions (PDF). This material is available free of charge via the Internet at <http://pubs.acs.org>.

AUTHOR INFORMATION

Corresponding Author

*E-mail: fabioc@qi.fcen.uba.ar; roitberg@ufl.edu.

Notes

The authors declare no competing financial interest.

ACKNOWLEDGMENTS

We dedicate this paper to Fred Wudl, with admiration. Financial support from UBACyT (grant X057), ANPCyT (PICT 25409), and Conicet (PIP 0877) is acknowledged. M.A.C. thanks Conicet for a doctoral fellowship. F.D.C. is a member of the scientific staff of Conicet. Computer resources were provided by the Large Allocations Resource Committee to A.E.R. The authors acknowledge the University of Florida High-Performance Computing Center (URL: <http://hpc.ufl.edu>) for providing computational resources and support that have contributed to the research results reported within this paper.

REFERENCES

- (1) Kellog, G. E.; Gaudiello, J. G. In *Inorganic Materials*, 2nd ed.; Bruce, D. W., O'Hare, D., Eds.; John Wiley & Sons Ltd.: Chichester, U. K., 1996.
- (2) Kitagawa, H.; Onodera, N.; Sonoyama, T.; Yamamoto, M.; Fukawa, T.; Mitani, T.; Seto, M.; Maeda, Y. *J. Am. Chem. Soc.* **1999**, *121*, 10068.
- (3) Delgado, S.; Sanz Miguel, P. J.; Priego, J. L.; Jimenez-Aparicio, R.; Gomez-García, C. J.; Zamora, F. *Inorg. Chem.* **2008**, *47*, 9128.
- (4) (a) Mitsumi, M.; Yoshida, Y.; Kohyama, A.; Kitagawa, Y.; Ozawa, Y.; Kobashashi, M.; Toriumi, K.; Tadokoro, M.; Ikeda, N.; Okumura,

- M.; Kurmoo, M. *Inorg. Chem.* **2009**, *48*, 6680. (b) Thabbokt, Z.; López, X.; de Graaf, C.; Guihéry, N.; Suaud, N.; Benamor, N. J. *Comput. Chem.* **2012**, *33*, 1748.
- (5) Yamashita, M.; Takaishi, S.; Kobashashi, A.; Kitagawa, H.; Matsuzaki, H.; Okamoto, H. *Coord. Chem. Rev.* **2006**, *250*, 2335.
- (6) (a) Kitagawa, S.; Noro, S. In *Compr. Coord. Chem.*; McCleverty, J., Meyer, T. J., Eds.; Elsevier Pergamon: Amsterdam, 2004; Vol. 7, p 231. (b) Constable, E. C. In *Compr. Coord. Chem.*; McCleverty, J., Meyer, T. J., Eds.; Elsevier Pergamon: Amsterdam, 2004; Vol. 7, p 263.
- (7) (a) Hanack, M.; Deger, S.; Lange, A. *Coord. Chem. Rev.* **1988**, *83*, 115. (b) Schneider, O.; Hanack, M. *Angew. Chem., Int. Ed. Engl.* **1983**, *95*, 804. (c) Hanack, M.; Lange, A.; Grosshans, R. *Synth. Met.* **1991**, *45*, 59. (d) Hanack, M.; Gül, A.; Subramanian, L. R. *Inorg. Chem.* **1992**, *31*, 1542. (e) Pohmer, J.; Hanack, M.; Barcina, O. *J. Mater. Chem.* **1996**, *6*, 957. (f) Hanack, M.; Lang, M. *Adv. Mater.* **1994**, *6*, 819.
- (8) Katz, M. J.; Kaluarachchi, H.; Batchelor, R. J.; Bokov, A. A.; Ye, Z. G.; Leznoff, D. B. *Angew. Chem., Int. Ed.* **2007**, *46*, 8804.
- (9) Olea, D.; Alexandre, S. S.; Amo-Ochoa, P.; Guijarro, A.; de Jesús, F.; Soler, J. M.; de Pablo, P. J.; Zamora, F.; Gómez-Herrero, J. *Adv. Mater.* **2005**, *17*, 1761.
- (10) Mas-Balleste, R.; Gonzalez-Prieto, R.; Guijarro, A.; Fernandez-Vindel, M. A.; Zamora, F. *Dalton Trans.* **2009**, 7341–7343.
- (11) Welte, L.; Calzolari, A.; Di Felice, R.; Zamora, F.; Gomez-Herrero, J. *Nat. Nanotechnol.* **2010**, *5*, 110.
- (12) Welte, L.; Gonzalez-Prieto, R.; Olea, D.; Torres, M. R.; Priego, J. L.; Jimenez-Aparicio, R.; Gomez-Herrero, J.; Zamora, F. *ACS Nano* **2008**, *2*, 2051.
- (13) (a) Aquino, M. A. S. *Coord. Chem. Rev.* **1998**, *170*, 141. (b) Aquino, M. A. S. *Coord. Chem. Rev.* **2004**, *248*, 1025.
- (14) Angaridis, P. In *Multiple Bonds between Metal Atoms*, 3rd ed.; Cotton, F. A., Murillo, C. A., Walton, R. A., Eds.; Springer Science and Business Media Inc.: New York, 2005; p 377.
- (15) (a) Arribas, G.; Barral, M. C.; Gonzalez-Prieto, R.; Jimenez-Aparicio, R.; Priego, J. L.; Torres, M. R.; Urbanos, F. A. *Inorg. Chem.* **2005**, *44*, 5770. (b) Kuwahara, R.; Fujikawa, S.; Kuroiwa, K.; Kimizuka, N. *J. Am. Chem. Soc.* **2012**, *134*, 1192.
- (16) (a) Chaia, Z.; Rusjan, M.; Castro, M. A.; Donnio, B.; Heinrich, B.; Guillon, D.; Baggio, R.; Cukiernik, F. D. *J. Mater. Chem.* **2009**, *19*, 4981. (b) Rusjan, M.; Donnio, B.; Heinrich, B.; Cukiernik, F. D.; Guillon, D. *Langmuir* **2002**, *18*, 10116. (c) Cukiernik, F. D.; Ibn-Elhaj, M.; Chaia, Z.; Marchon, J. C.; Giroud-Godquin, A. M.; Guillon, D.; Skoulios, A.; Maldivi, P. *Chem. Mater.* **1998**, *10*, 83. (d) Caplan, J. F.; Murphy, C. A.; Swansburg, S.; Lemieux, R. P.; Cameron, T. S.; Aquino, M. A. S. *Can. J. Chem.* **1998**, *76*, 1520.
- (17) Rossi, L.; Marceca, E.; Vega, D.; Cukiernik, F. D. *Proceedings of the XVII Congreso Argentino de Fisicoquímica y Química Inorgánica*, Argentina, 2011.
- (18) Giroud-Godquin, A. M.; Maldivi, P.; Marchon, J. C.; Aldebert, P.; Péguy, A.; Guillon, D.; Skoulios, A. *J. Phys. (Paris)* **1989**, *50*, 513.
- (19) Barberá, J.; Lantero, I.; Moyano, S.; Serrano, J. L.; Elduque, A.; Gimenez, R. *Chem.—Eur. J.* **2010**, *16*, 14545.
- (20) Bursten, B. E.; Chisholm, M. H.; D'Acchioli, J. S. *Inorg. Chem.* **2005**, *44*, 5571.
- (21) Wesemann, J. L.; Chisholm, M. H. *Inorg. Chem.* **1997**, *36*, 3258–3267.
- (22) (a) Cummings, S. P.; Cao, Z.; Liskey, C. W.; Geanes, A. R.; Fanwick, P. E.; Hassell, K. M.; Ren, T. *Organometallics* **2010**, *29*, 2783. (b) Xi, B.; Xu, G. L.; Fanwick, P. E.; Ren, T. *Organometallics* **2009**, *28*, 2338.
- (23) Wesemann, J. L.; Chisholm, M. H.; Christou, G.; Foltling, K.; Huffman, J. C.; Samuels, J. A.; James, C. A.; Woodruff, W. H. *Inorg. Chem.* **1996**, *35*, 3643.
- (24) Cotton, F. A.; Felthouse, T. R. *Inorg. Chem.* **1980**, *19*, 328.
- (25) Morosin, B.; Hughes, R. C.; Soos, Z. G. *Acta Crystallogr., Sect. B* **1975**, *31*, 762.
- (26) Cukiernik, F. D.; Giroud-Godquin, A.-M.; Maldivi, P.; Marchon, J.-C. *Inorg. Chim. Acta* **1994**, *215*, 203.
- (27) Handa, M.; Yoshioka, D.; Mikuriya, M.; Hiromitsu, I.; Kasuga, K. *Mol. Cryst. Liq. Cryst.* **2002**, *376*, 257.
- (28) Cotton, F. A.; Felthouse, T. R. *Inorg. Chem.* **1981**, *20*, 600.
- (29) Cotton, F. A.; Kim, Y.; Ren, T. *Inorg. Chem.* **1992**, *31*, 2723.
- (30) Miyasaka, H.; Clerac, R.; Campos-Fernandez, C. S.; Dunbar, K. R. *J. Chem. Soc., Dalton Trans.* **2001**, 858.
- (31) Beck, E. J.; Drysdale, K. D.; Thompson, L. K.; Li, L.; Murphy, C. A.; Aquino, M. A. S. *Inorg. Chim. Acta* **1998**, 279, 121.
- (32) Yoshioka, D.; Mikuriya, M.; Handa, M. *Bull. Chem. Soc. Jpn.* **2004**, *77*, 2205.
- (33) (a) Telsler, J.; Drago, R. S. *Inorg. Chem.* **1984**, *23*, 3114. (b) Telsler, J.; Miskowski, V. M.; Drago, R. S.; Wong, N. M. *Inorg. Chem.* **1985**, *24*, 4765. (c) Cukiernik, F. D.; Marchon, J. C.; Luneau, D.; Maldivi, P. *Inorg. Chem.* **1998**, *37*, 3698.
- (34) Bonnet, L.; Cukiernik, F. D.; Maldivi, P.; Giroud-Godquin, A. M.; Marchon, J. C.; Ibn-Elhaj, M.; Guillon, D.; Skoulios, A. *Chem. Mater.* **1994**, *6*, 31.
- (35) Kaim, W. *Coord. Chem. Rev.* **2002**, *230*, 127.
- (36) Gustav, K.; Schmitt, C. J. *Z. Chem.* **1969**, *9*, 32.
- (37) Schilt, A. A.; Dunbar, W. E.; Gandrud, B. W.; Warren, S. E. *Talanta* **1970**, *17*, 649.
- (38) Herberhold, M.; Süß-Fink, M. *Z. Naturforsch.* **1976**, *31B*, 1489.
- (39) Schneider, O.; Hanack, M. *Angew. Chem., Int. Ed. Engl.* **1983**, *22*, 784.
- (40) Sauer, J.; Sustmann, R. *Angew. Chem., Int. Ed. Engl.* **1983**, *19*, 779.
- (41) Cacelli, I.; Campanile, S.; Denti, G.; Ferretti, A.; Sommovigo, M. *Inorg. Chem.* **2004**, *43*, 1379.
- (42) (a) Glöcke, M.; Kaim, W. *Angew. Chem., Int. Ed. Engl.* **1999**, *38*, 3072. (b) Glöcke, M.; Kaim, W.; Klein, A.; Roduner, E.; Hübner, G.; Zalis, S.; van Slageren, J.; Renz, F.; Güttlich, O. *Inorg. Chem.* **2001**, *40*, 2256.
- (43) Estiu, G.; Cukiernik, F. D.; Maldivi, P.; Poizat, O. *Inorg. Chem.* **1999**, *38*, 3030.
- (44) Kitagawa, Y.; Shoji, M.; Koizumi, K.; Kawakami, T.; Okumura, M.; Yamaguchi, K. *Polyhedron* **2007**, *26*, 2154.
- (45) Castro, M. A.; Roitberg, A. E.; Cukiernik, F. D. *Inorg. Chem.* **2008**, *47*, 4682.
- (46) Castro, M. A.; Rusjan, M.; Vega, D.; Peña, O.; Weyhermüller, T.; Cukiernik, F. D.; Slep, L. *Inorg. Chim. Acta* **2011**, *374*, 499.
- (47) (a) Frisch, M. J.; Trucks, G. W.; Schlegel, H. B.; Scuseria, G. E.; Robb, M. A.; Cheeseman, J. R.; Montgomery, J. A., Jr.; Vreven, T.; Kudin, K. N.; Burant, J. C.; Millam, J. M.; Iyengar, S. S.; Tomasi, J.; Barone, V.; Mennucci, B.; Cossi, M.; Scalmani, G.; Rega, N.; Petersson, G. A.; Nakatsuji, H.; Hada, M.; Ehara, M.; Toyota, K.; Fukuda, R.; Hasegawa, J.; Ishida, M.; Nakajima, T.; Honda, Y.; Kitao, O.; Nakai, H.; Klene, M.; Li, X.; Knox, J. E.; Hratchian, H. P.; Cross, J. B.; Bakken, V.; Adamo, C.; Jaramillo, J.; Gomperts, R.; Stratmann, R. E.; Yazyev, O.; Austin, A. J.; Cammi, R.; Pomelli, C.; Ochterski, J. W.; Ayala, P. Y.; Morokuma, K.; Voth, G. A.; Salvador, P.; Dannenberg, J. J.; Zakrzewski, V. G.; Dapprich, S.; Daniels, A. D.; Strain, M. C.; Farkas, O.; Malick, D. K.; Rabuck, A. D.; Raghavachari, K.; Foresman, J. B.; Ortiz, J. V.; Cui, Q.; Baboul, A. G.; Clifford, S.; Cioslowski, J.; Stefanov, B. B.; Liu, G.; Liashenko, A.; Piskorz, P.; Komaromi, I.; Martin, R. L.; Fox, D. J.; Keith, T.; Al-Laham, M. A.; Peng, C. Y.; Nanayakkara, A.; Challacombe, M.; Gill, P. M. W.; Johnson, B.; Chen, W.; Wong, M. W.; Gonzalez, C.; Pople, J. A. *Gaussian 03*, revision C.02; Gaussian, Inc.: Wallingford, CT, 2004. (b) Frisch, M. J.; Trucks, G. W.; Schlegel, H. B.; Scuseria, G. E.; Robb, M. A.; Cheeseman, J. R.; Scalmani, G.; Barone, V.; Mennucci, B.; Petersson, G. A.; Nakatsuji, H.; Caricato, M.; Li, X.; Hratchian, H. P.; Izmaylov, A. F.; Bloino, J.; Zheng, G.; Sonnenberg, J. L.; Hada, M.; Ehara, M.; Toyota, K.; Fukuda, R.; Hasegawa, J.; Ishida, M.; Nakajima, T.; Honda, Y.; Kitao, O.; Nakai, H.; Vreven, T.; Montgomery, J. A., Jr.; Peralta, J. E.; Ogliaro, F.; Bearpark, M.; Heyd, J. J.; Brothers, E.; Kudin, K. N.; Staroverov, V. N.; Kobayashi, R.; Normand, J.; Raghavachari, K.; Rendell, A.; Burant, J. C.; Iyengar, S. S.; Tomasi, J.; Cossi, M.; Rega, N.; Millam, J. M.; Klene, M.; Knox, J. E.; Cross, J. B.; Bakken, V.; Adamo, C.; Jaramillo, J.; Gomperts, R.; Stratmann, R. E.; Yazyev, O.; Austin, A. J.; Cammi, R.; Pomelli, C.; Ochterski, J. W.; Martin, R. L.; Morokuma, K.; Zakrzewski, V. G.; Voth, G. A.; Salvador, P.;

Dannenberg, J. J.; Dapprich, S.; Daniels, A. D.; Farkas, Ö.; Foresman, J. B.; Ortiz, J. V.; Cioslowski, J.; Fox, D. J. *Gaussian 09*, revision A.1; Gaussian, Inc.: Wallingford, CT, 2009.

(48) (a) Becke, A. D. *J. Chem. Phys.* **1988**, *84*, 4524. (b) Perdew, J. P. *Phys. Rev. B* **1986**, *33*, 8822. (c) Lee, C.; Yang, W.; Parr, R. G. *Phys. Rev. B* **1988**, *37*, 785. (d) Becke, A. D. *J. Chem. Phys.* **1993**, *98*, 5648.

(49) (a) Dunning, T. H., Jr.; Hay, P. J. In *Modern Theoretical Chemistry*; Schaefer, H. F., III, Ed.; Plenum Press: New York, 1977; Vol. 3. (b) Hay, P. J.; Wadt, W. R. *J. Chem. Phys.* **1985**, *82*, 270. (c) Wadt, W. R.; Hay, P. J. *J. Chem. Phys.* **1985**, *82*, 284. (d) Hay, P. J.; Wadt, W. R. *J. Chem. Phys.* **1985**, *82*, 299.

(50) Perdew, J. P.; Burke, K.; Ernzerhof, M. *Phys. Rev. Lett.* **1996**, *77*, 3865.

(51) Zhao, Y.; Truhlar, D. G. *Theor. Chem. Acc.* **2008**, *120*, 215.

(52) (a) Stratmann, R. E.; Scuseria, G. E.; Frisch, M. J. *J. Chem. Phys.* **1998**, *109*, 8218. (b) Bauernschmitt, R.; Ahlrichs, R. *Chem. Phys. Lett.* **1996**, *256*, 454. (c) Casida, M. E.; Jamorski, C.; Casida, K. C.; Salahub, D. R. *J. Chem. Phys.* **1998**, *108*, 4439.

(53) Gorelsky, S. I. *SWizard program revision 4.6*; York University: Toronto, Canada, 1998; <http://www.sg-chem.net/>.

(54) Flükiger, P.; Lüthi, H. P.; Portmann, S.; Weber, J. *MOLEKEL 4.0*; Swiss National Supercomputing Centre CSCS: Manno, Switzerland, 2000.

(55) (a) Noodleman, L. *J. Chem. Phys.* **1981**, *74*, 5737. (b) Noodleman, L.; Davidson, E. R. *Chem. Phys.* **1986**, *109*, 131.

(56) (a) Soda, T.; Kitagawa, Y.; Onishi, T.; Takano, Y.; Shigeta, Y.; Nagao, H.; Yoshioka, Y.; Yamaguchi, K. *Chem. Phys. Lett.* **2000**, *319*, 223. (b) Yamaguchi, K.; Takahara, Y.; Fueno, T. In *Applied Quantum Chemistry*; Smith, V. H., Ed.; Reidel: Dordrecht, The Netherlands, 1986, p 155. (c) Nishino, M.; Yamanaka, S.; Yoshioka, Y.; Yamaguchi, K. *J. Phys. Chem. A* **1997**, *101*, 705.

(57) Ruiz, E.; Cano, J.; Alvarez, S.; Alemany, P. *J. Comput. Chem.* **1999**, *20*, 1391.

(58) Sauer, J.; Heldmann, D. K.; Hetzenegger, J.; Krauthan, J.; Sichert, H.; Schuster, J. *Eur. J. Org. Chem.* **1998**, 2885.

(59) Maldivi, P.; Giroud-Godquin, A. M.; Marchon, J. C.; Guillon, D.; Skoulios, A. *Chem. Phys. Lett.* **1986**, *157*, 552.

(60) Forest, E.; Maldivi, P.; Marchon, J. C.; Virelizier, H. *Spectroscopy* **1987**, *5*, 129.

(61) Gorelsky, S. I. *AOMIX: Program for Molecular Orbital Analysis*; University of Ottawa: Ottawa, ON, Canada, 2009; <http://www.sg-chem.net/>.

(62) Gorelsky, S. I.; Lever, A. B. P. *J. Organomet. Chem.* **2001**, *635*, 187.